IGARSS 2024 - 2024 IEEE International Geoscience and Remote Sensing Symposium | 979-8-3503-6032-5/24/$31.00 ©2024 IEEE | DOI: 10.1109/IGARSS53475.2024.10640920

AZIMUTHAL DEPENDENCE OF CYGNSS WINDS IN TROPICAL CYCLONES

Daniel Pascual[1], Christopher Ruf[2] and Rajeswari Balasubramaniam[2]

[1]Deimos Space UK Ltd., AIRSPEED1,1st Floor, 151 Eight Street, Harwell, OX11 0RL, United Kingdom
[2]Climate and Space Science and Engineering Department, University of Michigan, Ann Arbor, MI, USA

ABSTRACT

This article investigates the performance of a new CYGNSS wind speed product dedicated for tropical cyclones named merged (MRG). First, it analyzes the azimuthal performance. Later, the impact of the swells left after by the cyclone is also analyzed. The reference winds are those from another new product named MAXSS, a multi-mission product that blends winds from different sensors. Results show a dependency of the MRG winds on the two analyzed parameters, paving the way for an eventual incorporation of them into the retrieval algorithm.

Index Terms— GNSS-R, wind speed, cyclone, azimuthal dependence.

1. INTRODUCTION

Global Navigation Satellite System-Reflectometry (GNSS-R) is an L-band remote sensing technology that uses the reflected GNSS signals as signals of opportunity [1]. The NASA mission CYclone GNSS (CYGNSS) was launch in 2018 with the objective of measuring winds in cyclones using forward-reflected GNSS-R signals. The mission provides a global wind speed product for Fully Developed Seas (FDS). However, as it will be explained below, it is not suitable for cyclones. The CYGNSS team also builds a product for Young Seas/Limited Fetch (YSLF) scenarios that could be used in cyclones. However, it is up to the user to know when to use one or another product. To encompass this, a dedicated new product for cyclones named merged (MRG) has been recently created [2]. This article investigates its performance over the cyclone quadrants relative to the cyclone heading. Finally, the impact of the wakes left after by the cyclone is also studied.

Over the ocean, the forward reflected GNSS power (concretely, the power dispersion at different delays and Doppler frequencies) is related to the L-band Mean Square Slope (MSS), which in turn, is related to the wind speed (see [1] and the references therein). The MSS is a measure of the surface roughness and is defined as the energy of the second derivative of the surface spectrum. The L-band MSS is a low-pass version of the MSS. The upper limit of the integral depends on the radar frequency, the wind speed and the inverse wave age, a dimensionless parameter that characterizes the stage of wave development.

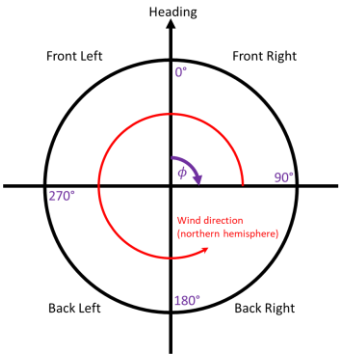


Figure 1: Schematic of a moving cyclone in the northern hemisphere. In the southern, the winds rotate clockwise.

In fully developed seas, the inverse wave age is low (ideally zero). In cyclone conditions, the relationship between wind speed and wave age becomes more complex due to the limited fetch (the distance over water that the wind blows in a single direction) and the translation motion of the cyclone (see Fig. 1). In principle, in a moving cyclone, the waves that propagate forward with the storm have a larger fetch than those that propagate in the opposite direction, and therefore, they are larger (e.g. [3]). In the northern hemisphere, the former waves are generated on the right half with respect to the cyclone heading, and the latter waves in the left half. The retrieval algorithm of the MRG winds does not consider this geometry dependency, or in other words, it is tuned to the average relationship between the sea surface roughness observed at L-band and the wind speed. It could be expected (and this is the motivation behind this work) that larger/lower waves for a given wind speed with respect to the average relationship between both would translate into an overestimation/underestimation of the winds by CYGNSS.

The azimuthal dependence of the L-band MSS was analyzed in [4] in four cyclones. The MSS was derived from the wind speed and the dominant wave period (from which the wave age can be obtained) measured with dropsondes from the National Oceanic and Atmospheric Administration (NOAA) hurricane missions. Next findings were emphasized: 1) the highest MSS are on the back right because the higher winds are generally in the right, and the young waves are in the back; 2) for the same wind speed, the MSS in the back half is larger than in the front half; and 3) this difference increases with increasing wind speed.

Authorized licensed use limited to: University of Michigan Library. Downloaded on December 04,2024 at 03:19:13 UTC from IEEE Xplore. Restrictions apply.

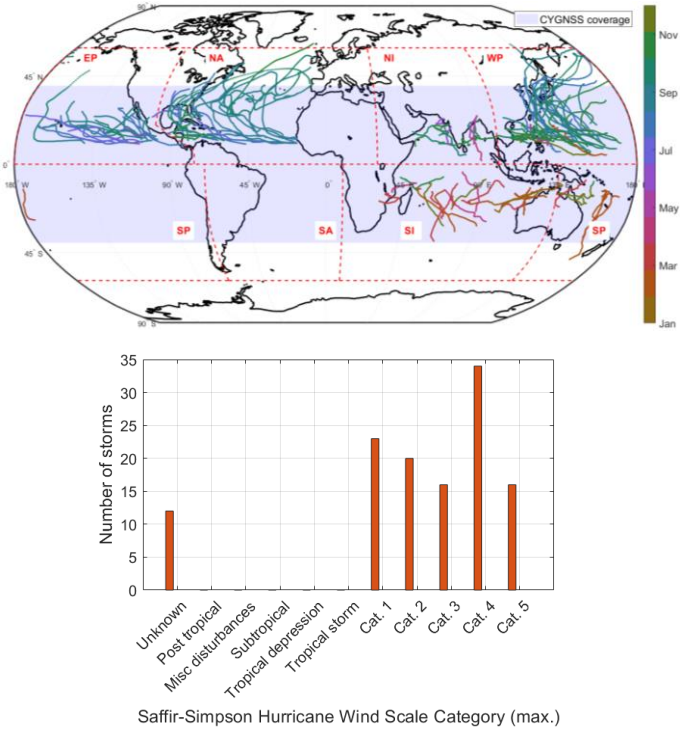


Figure 2: (top) trajectories and (bottom) categories of the cyclones used in this work. Acronyms denote the oceanic basins: South, North, East, West, Atlantic, Pacific & Indian.

Another study analyzed the dependence of CYGNSS L1 observables (which are later used in the wind speed retrieval) to cyclone winds [5]. The reference winds were those given by the NOAA Hurricane Weather Research Forecast (HWRF) model. It was found that for a given speed, there can be up to 8% variability in the L1 observables. As mentioned above, this variability comes from the fact the surface roughness to which the L-band is sensitive depends on the azimuth. This present article builds up on these findings but using the new CYGNSS MRG winds instead.

2. MATERIALS & METHODS

The CYGNSS MRG product is new L3 product that combines a dedicated L3 version of the YSLF winds (+/- 0.1 x 0.1 deg. from the storm center, +/- 6 hour) as the cyclone winds and the regular L3 FDS winds (0.2 x 0.2 deg., 1 hour) as the background winds [2]. The combination is performed in the spatial domain only (i.e. not considering the time before/after the cyclone has passed over a given area) with a tapered transition at the 34-knot radii as given the International Best Track Archive for Climate Stewardship (IBTrACS) project [6]. The MRG product is given in the form of an atlas of cyclones and is available at the Physical Oceanography Distributed Active Archive Center (PODAAC) [7]. Note that this first version is named v3.2, to denote that it uses the v3.2 of both FDS and YSLF winds.

The reference winds are obtained from the Marine Atmosphere eXtreme Satellite Synergy (MAXSS) project [8]. The MAXSS wind vectors are an L4 blended product (0.25 x 0.25 deg., 1 hour) obtained by spatially merging the winds from different sensors (ASCAT, SSMI/I, AMSR, SMAP, SMOS, GMI and Windsat) as the storm winds and the ERA5 winds as the background winds. The MAXSS winds are presented in the form of an atlas of 1131 storms (i.e. not only cyclones but subtropical and tropical storms as well) in the period 2010-2020, together with the associated IBTrACS data (storm position, radii, and translation speed among others) and other co-located data (e.g. SWH from sensors and models, sea surface height, precipitation, and many more).

This work analyzed 123 cyclones in the period 2018-2020. Their trajectories and maximum category as given by IBTrACS are shown in Fig. 2. The MAXXS winds are re-gridded over the CYGNSS coordinates (Lat. & Lon.) and times. IBTrACS data is linearly interpolated over the times.

3. RESULTS & DISCUSSION

3.1. Distribution of winds

Figure 3 shows the histograms of the MAXSS winds within the R_{34} knot radii in northern hemisphere cyclones. As it is well known in the field (e.g. [3]), the stronger winds can be observed in the right quadrants, particularly in the transition between the back and the front ($\phi = 90°$ in Fig. 1).

3.2. Overall performance

Figure 4 shows the joint histogram of the MRG and MAXSS winds. It can be observed a change on the distribution of the MAXSS winds around 34 knots, likely coming from the tapered transition between the FDS and YSLF winds around this point. It can also be observed that inside the cyclone, CYGNSS underestimates the winds with respect to MAXSS.

3.3. Azimuthal bias

Figure 5 shows the biases between the MAXSS and MRG winds within the R_{34} knot radii as a function of the azimuthal angle for different wind speed regimes.

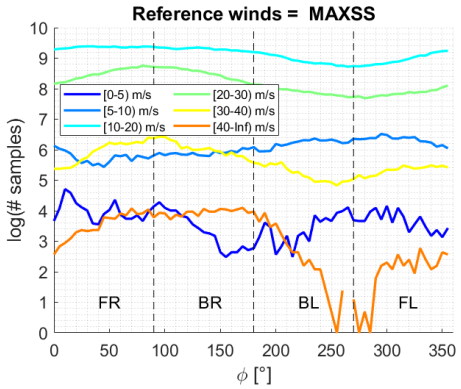


Figure 3: Wind speed histograms vs azimuth angle within the 34-knot radii.

Authorized licensed use limited to: University of Michigan Library. Downloaded on December 04,2024 at 03:19:13 UTC from IEEE Xplore. Restrictions apply.

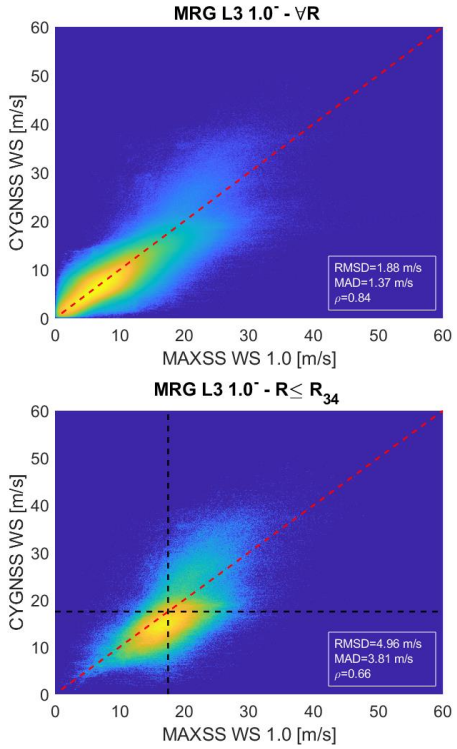


Figure 4: 2D log-histogram of MRG and MAXSS winds for (top) all radii and (bottom) within the 34-knot radii. Dashed black lines denote 34 knots (~17.5 m/s).

It can be observed that the biases have an harmonic dependence with the azimuth angle, and that their dynamic range increases with increasing the wind speed. This is consistent with [5], where a similar behavior is shown but with the L1 observables (which are later used to infer the wind speed). However, the harmonics of the wind biases are less clear. This is to be expected as the Geophysical Model Function (GMF) – the process by which the L1 observables are converted to wind speed - is optimized to the average relationship between some reference modelled winds (ERA5 for FDS and HWRF for YSLF) and those observables. In other words, the accuracy of a given wind speed is expected to be better in the cyclone areas where it is more common and worse elsewhere (compare Figs. 3 and 5 top).

The retrieval algorithm of the MRG winds incorporates a debiasing of the GMF winds on the sea state (which is included in the processing flow of both the YSLF and FDS winds [9]). In the algorithms, the sea state is characterized with modelled Significant Wave Height (SWH), which is defined as the energy of the surface spectrum. This sea state debasing helps in reducing the biases observed in Fig. 4. However, like the GMF design, the sea state debasing is optimized to the average relationship between winds and SWHs. This means that the accuracy of the MRG winds depends also on how close a given combination of winds and SWHs is to the most common one. Additionally, the modelled SWHs in cyclone conditions may not be as accurate as elsewhere.

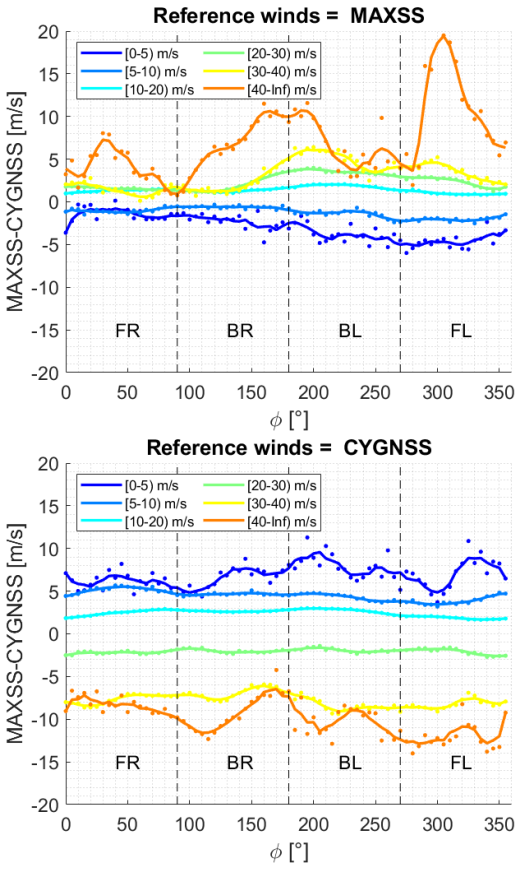


Figure 5: Azimuthal dependance of the bias for different wind speed regimes in the northern hemisphere.

Additionally, the spatial distribution of SWH is more complex than that of the winds [10]. Like the winds, larger waves (and therefore SWHs) are expected in the right quadrants. However, their degree of asymmetry is larger due to the complex combination of fetch and storm motion.

3.4. Cyclone swells

Waves generated by the cyclone will propagate out of their generating fetch into the ocean in the form of swells (e.g. [5]). Waves with a group velocity greater than the storm translation speed will propagate ahead. Waves with a lower group will be left behind. Swells can make the MRG product to overestimate the winds in areas far away from the cyclone due its use of the FDS winds as the background winds. Although the FDS product already includes a swell-correcting parameter [9], it uses reference data from a model, which may not quantify properly strong swells coming out from cyclones.

A possible example of this behavior is shown in Fig. 6. It can be observed in the top-right plot what it looks like a front-line of positive bias (i.e. CYGNSS overestimating the winds with respect to MAXSS) with a shape like the cyclone trajectory.

Authorized licensed use limited to: University of Michigan Library. Downloaded on December 04,2024 at 03:19:13 UTC from IEEE Xplore. Restrictions apply.

4. CONCLUSIONS AND FURTHER WORK

This work has shown that the performance of the MRG winds in tropical cyclones has an azimuthal dependence. Considering this in the retrieval algorithm was already suggested in [5], but at that time, the authors did not have enough co-locations with reference winds to build a robust retrieval algorithm. Additionally, it may also be interesting to consider building the product using a spatio-temporal merging of the FDS and YSLF winds (instead of only spatial) to encompass the impact of the swells left by the cyclones.

As further work, the authors plan to investigate the performance of the MRG winds depending on whether the cyclone is moving or steady; and to make triple co-locations with other wind sources, such as those from the HWRF model or from the Stepped Frequency Microwave Radiometer (SFMR) used in the NOAA flights. A triple co-location can be used to estimate the true error of a measurement, as a simple comparison between two systems (as done here) can lead to pseudobiases [11].

5. FUNDING

This research was jointly supported by the University of Michigan and by Deimos Space UK Limited, under the Contract SUBK00016056; by NASA Science Mission Directorate under Contract NNL13AQ00C with the University of Michigan; and by ESA under the contract 4000132954/20/I-NB Marine Atmosphere eXtreme Satellite Synergy (MAXSS) with Deimos Space UK Limited.

6. REFERENCES

[1] N. Rodriguez-Alvarez, J. F. Munoz-Martin, and M. Morris, "Latest Advances in the Global Navigation Satellite System—Reflectometry (GNSS-R) Field," Remote Sens., vol. 15, no. 8, p. 2157, Apr. 2023, doi: 10.3390/rs15082157.

[2] A. M. Warnock, C. S. Ruf, A. Russel, M. M. Al-Khaldi, and R. Balasubramaniam, "CYGNSS Level 3 Merged Wind Speed Data Product for Storm Force and Surrounding Environmental Winds," IEEE J. Sel. Top. Appl. Earth Obs. Remote Sens., pp. 1–13, 2024, doi: 10.1109/JSTARS.2024.3379934.

[3] I. Young, "A Review of Parametric Descriptions of Tropical Cyclone Wind-Wave Generation," Atmosphere (Basel)., vol. 8, no. 10, p. 194, Oct. 2017, doi: 10.3390/atmos8100194.

[4] P. A. Hwang, "Azimuthal Variation of L-Band Tilting Roughness Inside Tropical Cyclones," IEEE Geosci. Remote Sens. Lett., pp. 1–5, 2020, doi: 10.1109/LGRS.2020.3023655.

[5] R. Balasubramaniam and C. Ruf, "Azimuthal Dependence of GNSS-R Scattering Cross-Section in Hurricanes," J. Geophys. Res. Ocean., vol. 125, no. 7, Jul. 2020, doi: 10.1029/2020JC016167.

[6] Knapp, K. R., M. C. Kruk, D. H. Levinson, H. J. Diamond, and C. J. Neumann, 2010: The International Best Track Archive for Climate Stewardship (IBTrACS): Unifying tropical cyclone best track data. Bulletin of the American Meteorological Society, 91, 363-376. doi:10.1175/2009BAMS2755.1

[7] CYGNSS. 2024. CYGNSS Level 3 MRG Science Data Record Version 3.2. Ver. 3.2. PO.DAAC, CA, USA. Dataset accessed 2024-05-22 at https://doi.org/10.5067/CYGNS-L3M32

[8] MAXSS project webpage https://www.maxss.org/. Last accessed on 22/05/2024.

[9] D. Pascual, M. P. Clarizia, and C. S. Ruf, "Improved CYGNSS Wind Speed Retrieval Using Significant Wave Height Correction," Remote Sens., vol. 13, no. 21, p. 4313, Oct. 2021, doi: 10.3390/rs13214313.

[10] A. Tamizi and I. R. Young, "The Spatial Distribution of Ocean Waves in Tropical Cyclones," J. Phys. Oceanogr., vol. 50, no. 8, pp. 2123–2139, Aug. 2020, doi: 10.1175/JPO-D-20-0020.1.

[11] A. Stoffelen, "Toward the true near-surface wind speed: Error modeling and calibration using triple collocation," J. Geophys. Res. Ocean., vol. 103, no. C4, pp. 7755–7766, Apr. 1998, doi: 10.1029/97JC03180.

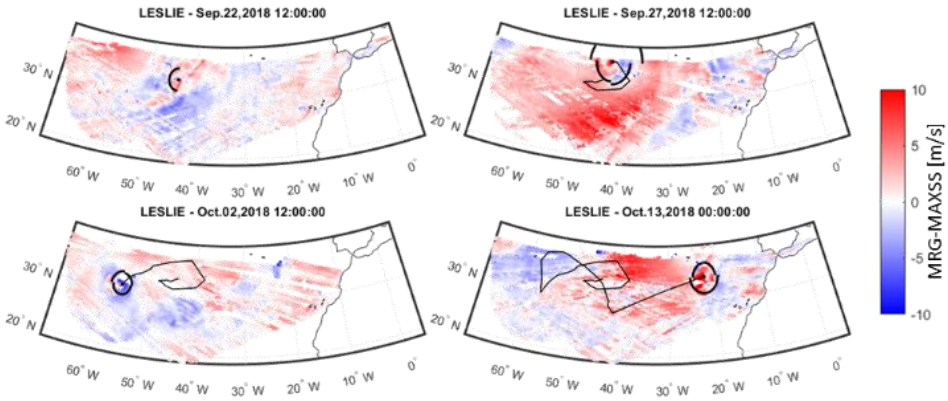


Figure 6: Bias in cyclone Leslie. Black lines and circles indicate the trajectory and the 34-knot radii respectively as given by IBTrACS

Authorized licensed use limited to: University of Michigan Library. Downloaded on December 04,2024 at 03:19:13 UTC from IEEE Xplore. Restrictions apply.